
ImageNet3D: Towards General-Purpose Object-Level 3D Understanding

Wufei Ma¹, Guanning Zeng², Guofeng Zhang¹, Qihao Liu¹, Letian Zhang³,
Adam Kortylewski^{4,5}, Yaoyao Liu¹, Alan L. Yuille¹

¹Johns Hopkins University ²Tsinghua University ³Tongji University
⁴University of Freiburg ⁵Max Planck Institute for Informatics

Abstract

A vision model with general-purpose object-level 3D understanding should be capable of inferring both 2D (e.g., class name and bounding box) and 3D information (e.g., 3D location and 3D viewpoint) for arbitrary rigid objects in natural images. This is a challenging task, as it involves inferring 3D information from 2D signals and most importantly, generalizing to rigid objects from unseen categories. However, existing datasets with object-level 3D annotations are often limited by the number of categories or the quality of annotations. Models developed on these datasets become specialists for certain categories or domains, and fail to generalize. In this work, we present ImageNet3D, a large dataset for general-purpose object-level 3D understanding. ImageNet3D augments 200 categories from the ImageNet dataset with 2D bounding box, 3D pose, 3D location annotations, and image captions interleaved with 3D information. With the new annotations available in ImageNet3D, we could (i) analyze the object-level 3D awareness of visual foundation models, and (ii) study and develop general-purpose models that infer both 2D and 3D information for arbitrary rigid objects in natural images, and (iii) integrate unified 3D models with large language models for 3D-related reasoning.. We consider two new tasks, probing of object-level 3D awareness and open vocabulary pose estimation, besides standard classification and pose estimation. Experimental results on ImageNet3D demonstrate the potential of our dataset in building vision models with stronger general-purpose object-level 3D understanding.

1 Introduction

General-purpose object-level 3D understanding requires models to infer both 2D (e.g., class name and bounding box) and 3D information (e.g., 3D location and 3D viewpoint) for arbitrary rigid objects in natural images. Correctly predicting these 2D and 3D information is crucial to a wide range of applications in robotics [1, 2] and general-purpose artificial intelligence [3, 4, 5]. Despite the success of previous learning-based approaches [6, 7], embodied or multi-modal LLM agents with stronger 3D awareness will not only reason and interact better with the 3D world [8, 9], but also alleviate certain key limitations, such as shortcut learning [10] or hallucination [11, 12].

Despite the importance of object-level 3D understanding, previous datasets in this area were limited to a very small number of categories [13, 14, 15] or specific domains, such as autonomous driving [16, 17] or indoor furniture [18]. Subsequent works then focused on developing specialized models that excel at 3D tasks for the categories and domains considered in these datasets. While these specialized models are found useful for certain downstream applications, they fail easily when generalizing to novel categories. It is largely understudied of how to develop unified 3D models that are capable of inferring 2D and 3D information for all common rigid objects in natural images.

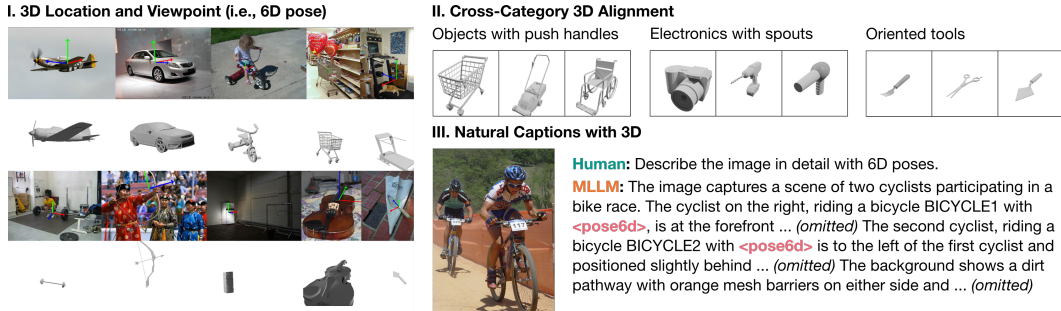


Figure 1: **Overview of ImageNet3D data and annotations.** ImageNet3D provides **3D location and viewpoint (i.e., 6D pose)** for more than 86,000 objects. We also annotate **cross-category 3D alignment** for the 200 rigid categories in ImageNet3D. Lastly we generate **image captions interleaved with 3D information** to integrate unified 3D models with large language models.

In the following, we consider two types of unified 3D models. **(i) Pretrained vision encoders with object-level 3D awareness.** Vision encoders from DINO [19], CLIP [20], Stable Diffusion [21], etc. are pretrained with self-supervised or weakly-supervised objectives. By learning a 3D discriminative representation, these vision encoders can be integrated into vision systems and benefit downstream recognition and reasoning. *While these encoders are found useful for 3D-related dense prediction tasks [22], their object-level 3D awareness remains unclear.* **(ii) Supervised 3D models.** By training on a large number of diverse data with 3D annotations, these models may achieve a stronger robustness and generalization ability. **However, there has been a lack of large-scale 3D datasets with a wide range of rigid categories, which constrains us from developing large unified 3D models for rigid objects or study the generalization and emerging properties of these models.**

In this work, we present ImageNet3D, a large dataset for general-purpose object-level 3D understanding. We extend 200 categories from ImageNet21k [23] with 2D bounding box and 6D pose annotations for more than 86,000 objects. To facilitate research on the two problems introduced above, ImageNet3D incorporates three key designs (see Figure 1). **(i) A large number of categories and instances.** ImageNet3D presents 2D and 3D annotations for a large number of object instances from a wide range of common rigid object categories found in natural images, as opposed to previous datasets focusing on specific categories and domains (see Table 1). This allows us to train and evaluate large unified 3D models capable of inferring both 2D and 3D information for arbitrary rigid objects. **(ii) Cross-category 3D alignment.** We align the canonical poses of all 200 categories based on semantic parts, shapes, and common knowledge, as shown in Figure 2. This is crucial for models to benefit from joint learning from multiple categories and to generalize to unseen categories, while omitted in previous datasets [24]. **(iii) Natural captions with 3D information.** We adopt a GPT-assisted approach [6] and produce image captions interleaved with 3D information. These captions will be valuable assets to integrate unified 3D models with large language models [25, 26] and perform 3D-related reasoning from natural images and language.

With the three key designs and new 3D annotations collected, ImageNet3D distinguishes itself from all previous 3D datasets and facilitates the evaluation and research of general-purpose object-level 3D understanding. Besides standard classification and pose estimation as studied in previous works [13, 24], we further consider two new tasks, probing of object-level 3D awareness and open-vocabulary pose estimation. Experimental results show that with ImageNet3D, we can develop general-purpose models capable of inferring 3D information for a wide range of rigid categories. Moreover, baseline results on ImageNet3D reveal the limitations of current 3D approaches and present new problems and challenges for future studies.

2 Related Works

Datasets with 3D annotations. Previous datasets with 3D annotations have led to significant advancements of 3D models for 3D object detection [29, 30] and pose estimation [31, 32, 14]. However, most existing datasets are limited to a small number of categories [13, 14, 15] or specific domains, such as autonomous driving [16, 17] or indoor furniture [18]. ObjectNet3D [24] extends the

Dataset	Images	# categories	# instances	Annotations
PASCAL3D+ (2014) [13]	Real	12	12,000	6D pose
ObjectNet3D (2016) [24]	Real	100	57,000	6D pose
CAMERA25 (2019) [27]	Synthetic	6	1,000	3D bbox
REAL275 (2019) [27]	Real	6	24	3D bbox
Objectron (2021) [28]	Real	9	18,000	3D bbox
Wild6D (2022) [14]	Real	5	2,000	3D bbox
ImageNet3D (ours)	Real	200	86,000	6D pose, captions, object visual quality, cross-category 3D alignment

Table 1: **Comparison between ImageNet3D and previous datasets with 3D annotations.** Previous datasets are limited by the number of rigid categories [13, 28, 14] or the quality of the annotations [24], constraining the development of large unified 3D models for general-purpose 3D understanding.

number of categories but the quality of the annotations constrains us from developing large unified 3D models. Our ImageNet3D largely extends the number of categories and instances, improves the annotation quality, and presents other crucial annotations such as cross-category 3D alignment and natural captions interleaved with 3D information. ImageNet3D allows us to develop unified 3D models for general-purpose 3D understanding and facilitates studies on new research problems, such as probing of object-level 3D awareness and open-vocabulary pose estimation.

Category-level pose estimation. Our work is closely related to category-level pose estimation, where a model predicts 3D or 6D poses for arbitrary instances from certain rigid categories. Previous works have explored keypoint-based methods [31] and 3D compositional models [32, 33]. However, these approaches limited their scopes to a small number of categories, and as far as we know, there were no attempts to develop large unified models for all common rigid categories. We further consider open-vocabulary pose estimation where models generalize to similar but novel categories. This topic has also been discussed in recent parallel works [34, 35] but [35] was limited to synthetic data rendered with photorealistic CAD models.

3D awareness of visual foundation Models. Recent work demonstrates the significant capabilities of large-scale pretrained vision models in 2D tasks [20, 36, 37, 38, 21], suggesting robust 2D representations. Beyond benchmarking the semantic and localization capabilities of visual backbones [39, 40, 41, 42, 43, 44], Banani et al. [22] studied the 3D awareness of these 2D models using trainable probes and zero-shot inference methods. However, their exploration was limited to only two basic aspects of 3D understanding – single-view surface reconstruction and multi-view consistency – due to absence of large datasets with 3D annotations. We further analyze the 3D awareness of visual models and provide a more comprehensive understanding of their progress in learning about the 3D structure of the world, demonstrating the significance of our proposed ImageNet3D.

3 ImageNet3D Dataset

ImageNet3D dataset aims to facilitate the evaluation and research of general-purpose object-level 3D understanding models. Besides 6D pose annotations for more than 86,000 objects from 200 categories, we annotate meta-classes, cross-category 3D alignment, and natural captions interleaved with 3D information as demonstrated in Figure 1. We start by presenting our dataset construction in Section 3.1. Then in Section 3.2 we introduce the necessity of cross-category 3D alignment and how it is achieved in our dataset. Lastly, we provide details on our image caption generation in Section 3.3.

3.1 Dataset Construction

Overview. We choose the ImageNet21k dataset [23] as our data source, as it provides a large and diverse set of images with class labels. We start by annotating 2D bounding boxes for the object instances in the images. We adopt a machine-assisted approach for 2D bounding box annotations, where a Grounding DINO model [45] is used to produce 2D bounding boxes prompted with the category label. The bounding box annotations are then filtered and improved by human evaluators. Next, we collect 3D CAD models as representative shapes for each object category from Objaverse [46].

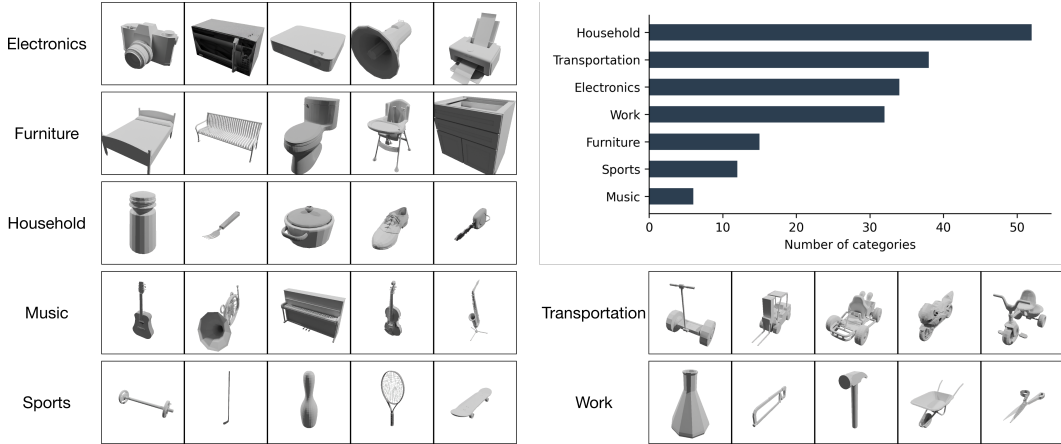


Figure 2: **Meta classes and cross-category 3D alignment.** We align the canonical poses of all 200 categories based on semantic parts, shapes, and common knowledge. This is crucial for models to benefit from joint learning from multiple categories and to generalize to novel categories.

The CAD models are carefully aligned based on their semantic parts and provide canonical poses for 6D pose annotations. Finally, we recruit a total of 30 annotators to annotate 6D poses for the objects, as well as the scene density and object visual quality.

Object categories. Our goal is to provide 3D annotations for all common rigid categories in real world. To achieve this, we carefully examine previous 2D and 3D datasets for image classification [23], object detection [47, 29, 28], and pose estimation [24, 27]. We choose the categories that are rigid, have well-defined shapes with certain variance, and have enough number of images available, which leads to the 200 categories in ImageNet3D. For detailed discussions on the choice of categories, please refer to Section A.1. Moreover, to leverage existing research in the field, we adopt the 100 categories and raw images from ObjectNet3D [24] and largely extend the number of categories and instances. As one of our goals is to improve the quality of 3D annotations, we only take unannotated images from ObjectNet3D, and all 3D annotations on these images are our original work. In Section E, we perform human evaluation on the annotation qualities in ObjectNet3D [24] and our ImageNet3D.

Annotator recruitment. We recruit 30 annotators for data annotation. To improve the quality of the collected data, each annotator must complete an onboarding stage before starting. The onboarding stage includes training sessions where we present detailed instructions of various annotations and proper ways to handle boundary cases. Additionally, each annotator must annotate sample questions and meet the accuracy threshold to qualify for subsequent work. Please refer to Section A and Section D regarding our annotator guidelines, training sessions, and ethics statement.

Data collection. We develop a web-based tool for data annotation so annotators can easily access the platform without local installation. A screenshot of our annotation tool is shown in Figure 4. For each object in ImageNet3D, the annotator needs to annotate the following. **(i) 3D location and 3D viewpoint (i.e., 6D pose):** For more intuitive annotating, the 3D location is parameterized as a combination of 2D location and distance of the object. The 3D viewpoint is defined as the rotation of the object with respect to the canonical pose of the category, and represented by three rotation parameters, azimuth, elevation, and in-plane rotation. **(ii) Density of the scene:** A binary label indicating if the scene is dense with many objects from the same category close to each other. **(iii) Visual quality of the object:** A categorical label with one of the four options: good, partially visible, barely visible, not visible. We refer the readers to Section D where we provide links to our annotation guidelines and instructions.

3.2 Cross-Category 3D Alignment

As explained in Section 3.1, the 3D viewpoint of an object is defined as the rotation of the object with respect to the canonical pose of this category. However, in previous datasets such as ObjectNet3D [24], canonical poses from different categories are not necessarily “aligned”. From the canonical poses



Figure 3: Mis-aligned canonical poses in ObjectNet3D [24].



Figure 4: Screenshot of our web app for data annotation.

depicted in Figure 3, the parts where the pencils “write” or the paintbrushes “paint” are pointing to different directions, and the spouts of faucets and kettles are also mis-aligned.

As we scale up the number of categories in 3D-annotated datasets, having cross-category 3D alignment is a crucial design for the study of general-purpose object-level 3D understanding. While objects from different categories have their unique characteristics, certain semantic parts are often shared between multiple categories, such as the wheels of “ambulances” and “forlifts” or push handles of “shopping carts” and “hand mowers”. Correctly aligning the canonical poses will (i) allow models to utilize the semantic similarities between parts of different categories and exploit the benefits of joint learning from multiple categories, and (ii) generalize to novel categories by inferring 3D viewpoints from semantic parts that the model has seen from other categories during training.

Therefore, we manually align the canonical poses of all 200 categories in ImageNet3D. Specifically, we consider the following three rules. **(i) Semantic parts:** categories sharing similar semantic parts, such as wheels, push handles, or spouts, should be aligned. **(ii) Similar shapes:** categories sharing similar shapes, such as fans, Ferris wheels, and life buoys, should be aligned. **(iii) Common knowledge:** certain categories are pre-defined with a “front” direction from common knowledge, such as “refrigerator”, “treadmill”, or “violin”.

3.3 Natural Captions with 3D Information

An important application of general-purpose object-level 3D understanding models is to integrate them with large language models (LLMs) and benefit downstream multi-modal reasoning. This would largely improve the 3D-awareness of multi-modal large language models (MLLMs) and improve 3D-related reasoning capabilities, such as poses [9] and distances [48]. Previous approaches integrated segmentation or human pose modules with MLLMs [25, 26] and demonstrate strong multi-modal reasoning abilities.

To integrate general-purpose 3D understanding with existing MLLMs, we present image captions interleaved with 3D information. As shown in Figure 1, our captions provide a detailed description of the image, object appearances and locations, as well as mutual relations. Moreover, for objects with 3D annotations, we add a special <pose6d> token as a reference to our 2D and 3D annotations for this object. To generate these image captions with 3D information, we adopt a GPT-assisted approach [6] and feed 2D and 3D annotations to the model via the textual prompts. Then GPT-4v is used to integrate these information and produce a coherent image caption interleaved with 3D information. Please refer to Section A.3 for details on caption generation as well as our GPT-4v prompts.

4 Tasks

With the new data and annotations available in ImageNet3D, we hope to push forward the evaluation and research of general-purpose object-level 3D understanding. We consider two new tasks, probing of 3D object-level awareness 4.1 and open-vocabulary pose estimation 4.2, besides joint image classification and category-level pose estimation 4.3.

4.1 Linear Probing of Object-Level 3D Awareness

Recent developments of large-scale pretraining have yielded visual foundation models with strong capabilities. Self-supervised approaches such as MAE [49] and DINO [19] provide strong and generalizable feature representations that benefit downstream recognition and localization. When jointly trained with language supervision, CLIP features [20] demonstrate transferability to a wide range of multi-modal tasks. Moreover, foundation models for specific tasks, e.g., MiDaS [50] for depth estimation, also show impressive capabilities when applied to arbitrary images.

Are these visual foundation models object-level 3D aware? Can these feature representations distinguish objects from different 3D viewpoints or retrieve objects from similar 3D viewpoints? Previous study [22] found that certain foundation models have better 3D awareness despite trained without 3D supervision. However, they focused on low-level tasks such as depth estimation and part correspondence. It remains unclear if these visual foundation models are object-level 3D aware and produce 3D discriminative object representations.

In this task, we aim to evaluate the object-level 3D awareness of visual foundation models by linear probing the frozen feature representations on 3D viewpoint classification task. This is because models with superior object-level 3D awareness would produce 3D discriminative features that help to classify the viewpoints correctly. Compared to low-level tasks such as depth estimation and part correspondence, object-level 3D awareness is directly associated with high-level scene understanding that is crucial to downstream recognition and reasoning in robotics and visual question answering.

Task formulation. We evaluate object-level 3D awareness by linear probing the frozen feature representations on 3D viewpoint classification task. Specifically, three linear classifiers are trained with respect to each of the three parameters encoding 3D viewpoint. Following the linear probing setting on ImageNet1k [51], we apply grid search to a range of hyperparameters, such as learning rate, pooling strategy, and training epochs, and select the best performance achievable with the frozen backbone features.

Evaluation. To jointly evaluate the classification results on three viewpoint parameters, we adopt the **pose error** given by the angle between the predicted rotation matrix and the groundtruth rotation matrix [31]

$$\Delta(R_{\text{pred}}, R_{\text{gt}}) = \frac{\|\logm(R_{\text{pred}}^{\top} R_{\text{gt}})\|_{\mathcal{F}}}{\sqrt{2}} \quad (1)$$

Based on the pose errors, we compute **pose estimation accuracy**, which is the percentage of samples with pose errors smaller than a pre-defined threshold.

4.2 Open-Vocabulary Pose Estimation

Existing 3D models for pose estimation [31, 32, 14] or object detection [30, 29] focused on scenarios where object images and 3D annotations from the target categories are available at training time. These models fail easily when generalizing to novel categories that possess similar semantic parts with categories that the models are trained on. A recent study [34] investigated the open-vocabulary pose estimation problem from synthetic data rendered with photorealistic CAD models. However, the synthetic dataset demonstrates limited variations in both object appearances and image backgrounds, while our ImageNet3D provide 3D annotations on real images from a wide range of rigid categories to study this problem.

How can 3D models generalize to novel categories? Intuitively models may utilize semantic parts that are shared between novel categories and categories that are seen during training. As demonstrated in Figure 5, models may generalize 3D knowledge learned from cars (*i.e.*, sedans and SUVs) to fire trucks based on the wheels and body of vehicles, or from hand barrows to shopping cars based on the push handles. Additionally, open-vocabulary pose estimation models may utilize large-scale 2D pre-training data or vision-language supervision and learn useful semantic information. For instance, after seeing 2D images of people riding a bicycle and a tricycle, models would learn to align the semantic parts and generalize from bicycles to tricycles. Lastly we provide detailed descriptions of object shape, part structure, and how humans interact with these objects for all categories in ImageNet3D (see Section A.1). Models may utilize such information and learn transferable features that generalize to novel rigid categories.

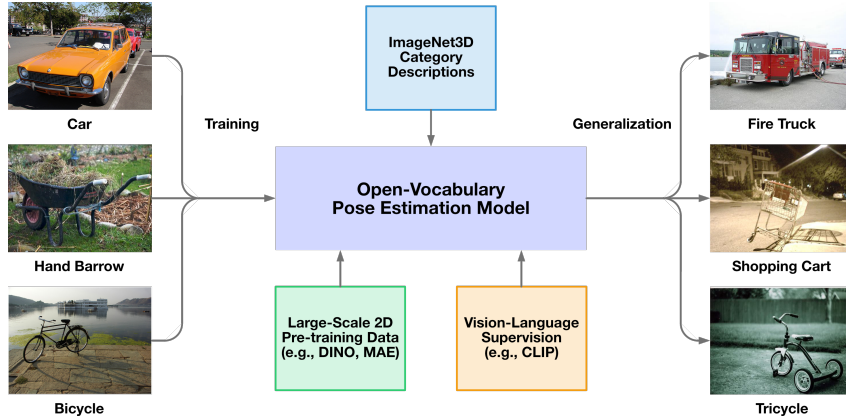


Figure 5: **Illustration of open vocabulary pose estimation.** Open-vocabulary models may utilize large-scale 2D data, vision-language supervision, or our category descriptions to learn transferable features and generalize to novel rigid categories.

Task formulation. We split the 200 categories in ImageNet to 63 common categories for training and 137 categories for open-vocabulary pose estimation. Models may utilize additional 2D data for pretraining but may be only trained on 3D annotations from the 63 common categories. During testing time, models have access to our annotated category-level captions besides the testing images. For complete lists of categories used for training and open-vocabulary pose estimation, please refer to Section D.

Evaluation. Following standard pose estimation tasks [13, 24], we report *pose estimation accuracy* and median *pose error* (Eq. 1) on testing data from novel rigid categories that are unseen during training.

4.3 Joint Image Classification and Category-Level Pose Estimation

For joint image classification and category-level pose estimation, a model first classifies the object and then predicts the 3D viewpoint of the object. A prediction is only considered correct if both the predicted class label is correct and the pose error is within a given threshold.

While this task has been studied in previous datasets [13, 24], ImageNet3D brings new challenges to existing models. Previous studies often focused on 12 or 20 categories [31, 32, 33] – how can we scale up these category-level 3D models to 200 categories while retaining a comparable performance? Moreover, with the meta classes and more categories available, we can better assess the limitations of current category-level pose estimation models.

Task formulation. For each of the 200 categories, we split the samples into training and validation splits, each accounting for about 50% of the data. Based on the number of samples used for training, we can further evaluate models under zero-shot, few-shot, and fully supervised settings.

Evaluation. Following [33], we adopt the **3D-aware classification accuracy**, where a prediction is correct only if the predicted class label is correct and the predicted pose error is lower than a given threshold.

5 Experimental Results

In this section we report the baseline performance of linear probing of object-level 3D awareness in Section 5.1, open-vocabulary pose estimation in Section 5.2, and joint image classification and category-level pose estimation in Section 5.3. For implementation details of various baseline models, including hyperparameters and hardware setup, please refer to Section C in the appendix. Note that after careful analysis, we find that annotations for a small number of categories are not accurate enough so they are sent back to the annotators for refinement. All experimental results in this section are based on data from **189 categories** of ImageNet3D.

Model	Arch.	Supervision	Dataset	Pose Acc@ $\pi/6$ \uparrow							
				Avg.	Elec.	Fur.	Hou.	Mus.	Spo.	Veh.	Work
DeiT III [52]	ViT-B/16	classification	ImageNet21k	36.6	47.9	48.2	36.8	21.5	16.6	35.0	25.3
MAE [49]	ViT-B/16	SSL	ImageNet1k	46.6	57.6	67.8	40.2	29.0	20.2	58.4	25.6
DINO [19]	ViT-B/16	SSL	ImageNet1k	42.0	53.1	57.0	39.8	28.0	19.3	45.3	27.0
DINO v2 [51]	ViT-B/14	SSL	LVD-142M	56.3	64.0	75.3	47.9	32.9	23.5	74.7	38.1
CLIP [20]	ViT-B/16	VLM	<i>private</i>	39.7	50.3	52.8	39.7	23.1	19.3	39.8	26.4
MiDaS [50]	ViT-L/16	depth	MIX-6	40.5	50.9	56.7	40.2	26.7	18.9	39.2	28.1

Table 2: **Quantitative results on probing of object-level 3D awareness.** We report the $\pi/6$ pose estimation accuracy for the average performance on all categories, as well as the performance for each meta class (from left to right): *electronics, furniture, household items, music instrument, sports equipment, vehicles & transportation, and work equipment*. Among the tested visual foundation models, DINO v2 demonstrated the best object-level 3D awareness.

5.1 Linear Probing of Object-Level 3D Awareness

Baselines. We measure the object-level 3D awareness for a range of general-purpose vision models designed for representation learning [52, 49, 19, 51], multi-modal learning [20], and depth estimation [50]. These models adopt standard transformer architectures and we train a linear probe on frozen class embedding features. We focus on model sizes comparable to ViT-base and report the training supervisions and datasets in Table 2.

Results. We report the pose estimation accuracies with threshold $\pi/6$ for various baseline methods in Table 2. Results show that visual foundation models trained without 3D supervision demonstrates a reasonable level of object-level 3D awareness. Specifically, we find that DINO v2 largely outperforms other approaches in terms of object-level 3D awareness, followed by MAE, DINO, and MiDaS. However, the gap between these models are much smaller than the findings in [22]. Our ImageNet3D provides valuable assets to assess these visual foundation models from the perspective of object-level 3D awareness. In Section F.1 we present results on different metrics and study the scaling properties of self-supervised approaches on object-level 3D awareness.

5.2 Open-Vocabulary Pose Estimation

Baselines. Open-vocabulary pose estimation is a rather new topic, and there are no existing baselines designed specifically for this task. Oryon [34] operates on RGBD data and requires an image of the same object from a different viewpoint as a reference. OV9D [35] studies the problem by generating photorealistic synthetic data but the code is not available for reproduction. Hence for baseline results, we consider models that learn category-agnostic features that generalize to novel categories and instances. Two types of approaches are considered: (i) **Classification-based methods** that formulate pose estimation as a classification problem. A pose classification head is trained on top of the backbone features. We consider two types of backbones, ResNet50 and Swin Transformer-Tiny, as our baselines. (ii) **3D compositional models** learn neural mesh models with contrastive features and perform analysis-by-synthesis during inference. We develop *NMM-Sphere*, which is a 3D compositional model with a general sphere mesh for all categories and trained with class and part contrastive features [33].

Results. We report the pose estimation accuracy with threshold $\pi/6$ in Table 3 and present the full results in Section F.2. Results show that by annotating cross-category 3D alignment, models trained with category-agnostic features can generalize to novel categories with a reasonable performance. However, generalization abilities of current 3D models are still quite limited when compared to models trained on annotations from novel categories. Open-vocabulary pose estimation is a rather new topic but is crucial to the development of general-purpose 3D understanding. We call for future studies on this challenging but important problem.

5.3 Image Classification and Category-Level Pose Estimation

Baselines. We consider two types of baseline methods: (i) **Classification-based methods** that formulate pose estimation as a classification problem and train a shared pose classification head.

Model	Novel Categories - Pose Acc@ $\pi/6$ \uparrow							
	Avg.	Electronics	Furniture	Household	Music	Sports	Vehicles	Work
ResNet50-General (trained on novel categories)	53.6	49.2	52.4	45.8	26.0	65.2	56.5	58.5
ResNet50-General	37.1	30.1	35.6	28.1	11.8	51.7	36.7	40.9
SwinTrans-T-General	<u>35.8</u>	<u>30.9</u>	<u>34.3</u>	<u>26.1</u>	<u>12.2</u>	<u>46.2</u>	<u>34.4</u>	<u>39.2</u>
NMM-Sphere	29.5	31.7	25.4	21.7	25.6	19.8	33.4	19.3

Table 3: **Quantitative results on open-vocabulary pose estimation.** We report the *pose estimation accuracy* with threshold $\pi/6$ on testing data from novel categories unseen during training. We report the average performance on all novel categories, as well as performance for novel categories in each meta class. Results show that models with category-agnostic features can generalize to novel categories, but by a limited amount.

Model	3D-Aware Acc@ $\pi/6$ \uparrow							
	Avg.	Electronics	Furniture	Household	Music	Sports	Vehicles	Work
ResNet50-General	50.9	60.0	<u>67.2</u>	43.0	43.8	27.7	64.1	33.8
SwinTrans-T-General	53.2	63.1	71.6	44.8	<u>45.3</u>	30.4	66.2	35.0
LLaVA-pose	49.1	58.0	65.6	41.6	41.0	26.1	61.8	32.1
NOVUM [33]	<u>56.2</u>	59.6	65.6	52.5	41.9	<u>30.6</u>	69.6	<u>39.3</u>
NMM-Sphere	57.4	<u>61.3</u>	65.9	<u>52.4</u>	51.7	40.5	<u>67.9</u>	43.4

Table 4: **Quantitative results on joint image classification and category-level pose estimation.** We report the *3D-aware classification accuracy* with threshold $\pi/6$ for the average performance, as well as performance for each meta class. Results show that with ImageNet3D, we can develop unified 3D models capable of inferring 3D information for a wide range of rigid categories. However, we also identify limitations of current 3D models when scaling up to a lot more object categories.

Following previous works [31, 33], we extend ResNet50 and Swin Transformer-Tiny for pose estimation, denoted by “ResNet50-General” and “SwinTrans-T-General”. **(ii) 3D compositional models** learn neural mesh models with contrastive features and perform analysis-by-synthesis during inference. NOVUM [33] adopts category-level meshes and more robust rendering techniques. We develop *NMM-Sphere*, which is a 3D compositional model with a general sphere mesh for all categories and is trained with class and part contrastive features [33].

Results. We report the 3D-aware classification accuracy with threshold $\pi/6$ in Table 4. Results show that with ImageNet3D, we can develop general-purpose models capable of inferring 3D information for a wide range of common rigid categories. However, we also note that there is a clear performance degradation as the number of categories scale up, as compared to results found in previous works [33]. We present the full results with other metrics and backbones and study the scaling properties of pose estimation models in Section F.3.

6 Conclusion

In this paper we present ImageNet3D, a large dataset for general-purpose object-level 3D understanding. ImageNet3D largely extends the number of rigid categories and object instances, as compared to previous datasets with 3D annotations. Moreover, ImageNet3D improves the quality of 3D annotations by annotating cross-category 3D alignment, and provides new types of annotations, such as object visual qualities and image captions interleaved with 3D information that enable new research problems. We provide baseline results on standard 3D tasks, as well as novel tasks such as probing of object-level 3D awareness and open-vocabulary pose estimation. Experimental results show that with ImageNet3D, we can develop general-purpose models capable of inferring 3D information for a wide range of rigid categories. We also identify limitations of existing 3D models from our baseline experiments and discuss new problems and challenges for future studies.

References

- [1] Abhishek Padalkar, Acorn Pooley, Ajinkya Jain, Alex Bewley, Alex Herzog, Alex Irpan, Alexander Khazatsky, Anant Rai, Anikait Singh, Anthony Brohan, et al. Open x-embodiment: Robotic learning datasets and rt-x models. *arXiv preprint arXiv:2310.08864*, 2023.
- [2] Chengshu Li, Ruohan Zhang, Josiah Wong, Cem Gokmen, Sanjana Srivastava, Roberto Martín-Martín, Chen Wang, Gabrael Levine, Wensi Ai, Benjamin Martinez, et al. Behavior-1k: A human-centered, embodied ai benchmark with 1,000 everyday activities and realistic simulation. *arXiv preprint arXiv:2403.09227*, 2024.
- [3] Erik Wijmans, Samyak Datta, Oleksandr Maksymets, Abhishek Das, Georgia Gkioxari, Stefan Lee, Irfan Essa, Devi Parikh, and Dhruv Batra. Embodied Question Answering in Photorealistic Environments with Point Cloud Perception. In *Proceedings of the IEEE Conference on Computer Vision and Pattern Recognition (CVPR)*, 2019.
- [4] Erik Wijmans, Samyak Datta, Oleksandr Maksymets, Abhishek Das, Georgia Gkioxari, Stefan Lee, Irfan Essa, Devi Parikh, and Dhruv Batra. Embodied question answering in photorealistic environments with point cloud perception. In *Proceedings of the IEEE/CVF Conference on Computer Vision and Pattern Recognition*, pages 6659–6668, 2019.
- [5] Arjun Majumdar, Anurag Ajay, Xiaohan Zhang, Pranav Putta, Sriram Yenamandra, Mikael Henaff, Sneha Silwal, Paul Mcvay, Oleksandr Maksymets, Sergio Arnaud, Karmesh Yadav, Qiyang Li, Ben Newman, Mohit Sharma, Vincent Berges, Shiqi Zhang, Pulkit Agrawal, Yonatan Bisk, Dhruv Batra, Mrinal Kalakrishnan, Franziska Meier, Chris Paxton, Sasha Sax, and Aravind Rajeswaran. Openeqa: Embodied question answering in the era of foundation models. In *Conference on Computer Vision and Pattern Recognition (CVPR)*, 2024.
- [6] Haotian Liu, Chunyuan Li, Qingyang Wu, and Yong Jae Lee. Visual instruction tuning. In *NeurIPS*, 2023.
- [7] Junnan Li, Dongxu Li, Silvio Savarese, and Steven Hoi. Blip-2: Bootstrapping language-image pre-training with frozen image encoders and large language models. In *International conference on machine learning*, pages 19730–19742. PMLR, 2023.
- [8] Zhuowan Li, Xingrui Wang, Elias Stengel-Eskin, Adam Kortylewski, Wufei Ma, Benjamin Van Durme, and Alan L Yuille. Super-clevr: A virtual benchmark to diagnose domain robustness in visual reasoning. In *Proceedings of the IEEE/CVF Conference on Computer Vision and Pattern Recognition*, pages 14963–14973, 2023.
- [9] Xingrui Wang, Wufei Ma, Zhuowan Li, Adam Kortylewski, and Alan L Yuille. 3d-aware visual question answering about parts, poses and occlusions. *Advances in Neural Information Processing Systems*, 36, 2024.
- [10] Mengnan Du, Fengxiang He, Na Zou, Dacheng Tao, and Xia Hu. Shortcut learning of large language models in natural language understanding. *Communications of the ACM*, 67(1):110–120, 2023.
- [11] Yiyang Zhou, Chenhang Cui, Jaehong Yoon, Linjun Zhang, Zhun Deng, Chelsea Finn, Mohit Bansal, and Huaxiu Yao. Analyzing and mitigating object hallucination in large vision-language models. *arXiv preprint arXiv:2310.00754*, 2023.
- [12] Wei Li, Zhen Huang, Houqiang Li, Le Lu, Yang Lu, Xinmei Tian, Xu Shen, and Jieping Ye. Visual evidence prompting mitigates hallucinations in multimodal large language models, 2024.
- [13] Yu Xiang, Roozbeh Mottaghi, and Silvio Savarese. Beyond pascal: A benchmark for 3d object detection in the wild. In *IEEE winter conference on applications of computer vision*, pages 75–82. IEEE, 2014.
- [14] Yang Fu and Xiaolong Wang. Category-level 6d object pose estimation in the wild: A semi-supervised learning approach and a new dataset. *Advances in Neural Information Processing Systems*, 35:27469–27483, 2022.
- [15] Bingchen Zhao, Shaozuo Yu, Wufei Ma, Mingxin Yu, Shenxiao Mei, Angtian Wang, Ju He, Alan Yuille, and Adam Kortylewski. Ood-cv: A benchmark for robustness to out-of-distribution shifts of individual nuisances in natural images. In *European conference on computer vision*, pages 163–180. Springer, 2022.

- [16] Andreas Geiger, Philip Lenz, and Raquel Urtasun. Are we ready for autonomous driving? the kitti vision benchmark suite. In *Conference on Computer Vision and Pattern Recognition (CVPR)*, 2012.
- [17] Holger Caesar, Varun Bankiti, Alex H Lang, Sourabh Vora, Venice Erin Liong, Qiang Xu, Anush Krishnan, Yu Pan, Giancarlo Baldan, and Oscar Beijbom. nuscenes: A multimodal dataset for autonomous driving. In *Proceedings of the IEEE/CVF conference on computer vision and pattern recognition*, pages 11621–11631, 2020.
- [18] Gilad Baruch, Zhuoyuan Chen, Afshin Dehghan, Tal Dimry, Yuri Feigin, Peter Fu, Thomas Gebauer, Brandon Joffe, Daniel Kurz, Arik Schwartz, and Elad Shulman. ARKitscenes - a diverse real-world dataset for 3d indoor scene understanding using mobile RGB-d data. In *Thirty-fifth Conference on Neural Information Processing Systems Datasets and Benchmarks Track (Round 1)*, 2021.
- [19] Mathilde Caron, Hugo Touvron, Ishan Misra, Hervé Jégou, Julien Mairal, Piotr Bojanowski, and Armand Joulin. Emerging properties in self-supervised vision transformers. In *Proceedings of the International Conference on Computer Vision (ICCV)*, 2021.
- [20] Alec Radford, Jong Wook Kim, Chris Hallacy, Aditya Ramesh, Gabriel Goh, Sandhini Agarwal, Girish Sastry, Amanda Askell, Pamela Mishkin, Jack Clark, et al. Learning transferable visual models from natural language supervision. In *International conference on machine learning*, pages 8748–8763. PMLR, 2021.
- [21] Robin Rombach, Andreas Blattmann, Dominik Lorenz, Patrick Esser, and Björn Ommer. High-resolution image synthesis with latent diffusion models. In *Proceedings of the IEEE/CVF conference on computer vision and pattern recognition*, pages 10684–10695, 2022.
- [22] Mohamed El Banani, Amit Raj, Kevis-Kokitsi Maninis, Abhishek Kar, Yuanzhen Li, Michael Rubinstein, Deqing Sun, Leonidas Guibas, Justin Johnson, and Varun Jampani. Probing the 3d awareness of visual foundation models. *arXiv preprint arXiv:2404.08636*, 2024.
- [23] Jia Deng, Wei Dong, Richard Socher, Li-Jia Li, Kai Li, and Li Fei-Fei. Imagenet: A large-scale hierarchical image database. In *2009 IEEE conference on computer vision and pattern recognition*, pages 248–255. Ieee, 2009.
- [24] Yu Xiang, Wonhui Kim, Wei Chen, Jingwei Ji, Christopher Choy, Hao Su, Roozbeh Mottaghi, Leonidas Guibas, and Silvio Savarese. Objectnet3d: A large scale database for 3d object recognition. In *Computer Vision—ECCV 2016: 14th European Conference, Amsterdam, The Netherlands, October 11–14, 2016, Proceedings, Part VIII 14*, pages 160–176. Springer, 2016.
- [25] Yao Feng, Jing Lin, Sai Kumar Dwivedi, Yu Sun, Priyanka Patel, and Michael J. Black. Chatpose: Chatting about 3d human pose. In *CVPR*, 2024.
- [26] Xin Lai, Zhuotao Tian, Yukang Chen, Yanwei Li, Yuhui Yuan, Shu Liu, and Jiaya Jia. Lisa: Reasoning segmentation via large language model. *arXiv preprint arXiv:2308.00692*, 2023.
- [27] He Wang, Srinath Sridhar, Jingwei Huang, Julien Valentin, Shuran Song, and Leonidas J Guibas. Normalized object coordinate space for category-level 6d object pose and size estimation. In *Proceedings of the IEEE/CVF Conference on Computer Vision and Pattern Recognition*, pages 2642–2651, 2019.
- [28] Adel Ahmadyan, Liangkai Zhang, Artsiom Ablavatski, Jianing Wei, and Matthias Grundmann. Objectron: A large scale dataset of object-centric videos in the wild with pose annotations. In *Proceedings of the IEEE/CVF Conference on Computer Vision and Pattern Recognition (CVPR)*, pages 7822–7831, June 2021.
- [29] Garrick Brazil, Abhinav Kumar, Julian Straub, Nikhila Ravi, Justin Johnson, and Georgia Gkioxari. Omni3D: A large benchmark and model for 3D object detection in the wild. In *CVPR*, Vancouver, Canada, June 2023. IEEE.
- [30] Peixuan Li, Huaici Zhao, Pengfei Liu, and Feidao Cao. Rtm3d: Real-time monocular 3d detection from object keypoints for autonomous driving, 2020.
- [31] Xingyi Zhou, Arjun Karapur, Linjie Luo, and Qixing Huang. Starmap for category-agnostic keypoint and viewpoint estimation. In *Proceedings of the European Conference on Computer Vision (ECCV)*, pages 318–334, 2018.

- [32] Wufei Ma, Angtian Wang, Alan Yuille, and Adam Kortylewski. Robust category-level 6d pose estimation with coarse-to-fine rendering of neural features. In *European Conference on Computer Vision*, pages 492–508. Springer, 2022.
- [33] Artur Jesslen, Guofeng Zhang, Angtian Wang, Alan Yuille, and Adam Kortylewski. Robust 3d-aware object classification via discriminative render-and-compare. *arXiv preprint arXiv:2305.14668*, 2023.
- [34] Jaime Corsetti, Davide Boscaini, Changjae Oh, Andrea Cavallaro, and Fabio Poiesi. Open-vocabulary object 6d pose estimation. 2024.
- [35] Junhao Cai, Yisheng He, Weihao Yuan, Siyu Zhu, Zilong Dong, Liefeng Bo, and Qifeng Chen. Ov9d: Open-vocabulary category-level 9d object pose and size estimation. *arXiv preprint arXiv:2403.12396*, 2024.
- [36] Alexander Kirillov, Eric Mintun, Nikhila Ravi, Hanzi Mao, Chloe Rolland, Laura Gustafson, Tete Xiao, Spencer Whitehead, Alexander C Berg, Wan-Yen Lo, et al. Segment anything. In *Proceedings of the IEEE/CVF International Conference on Computer Vision*, pages 4015–4026, 2023.
- [37] Xueyan Zou, Jianwei Yang, Hao Zhang, Feng Li, Linjie Li, Jianfeng Wang, Lijuan Wang, Jianfeng Gao, and Yong Jae Lee. Segment everything everywhere all at once. *Advances in Neural Information Processing Systems*, 36, 2024.
- [38] Junfeng Wu, Yi Jiang, Qihao Liu, Zehuan Yuan, Xiang Bai, and Song Bai. General object foundation model for images and videos at scale. *arXiv preprint arXiv:2312.09158*, 2023.
- [39] Micah Goldblum, Hossein Sourin, Renkun Ni, Manli Shu, Viraj Prabhu, Gowthami Somepalli, Prithvijit Chattopadhyay, Mark Ibrahim, Adrien Bardes, Judy Hoffman, et al. Battle of the backbones: A large-scale comparison of pretrained models across computer vision tasks. *Advances in Neural Information Processing Systems*, 36, 2024.
- [40] Priya Goyal, Dhruv Mahajan, Abhinav Gupta, and Ishan Misra. Scaling and benchmarking self-supervised visual representation learning. In *Proceedings of the IEEE/CVF International Conference on Computer Vision*, pages 6391–6400, 2019.
- [41] Martha Lewis, Nihal V Nayak, Peilin Yu, Qinan Yu, Jack Merullo, Stephen H Bach, and Ellie Pavlick. Does clip bind concepts? probing compositionality in large image models. *arXiv preprint arXiv:2212.10537*, 2022.
- [42] Zhuowan Li, Cihang Xie, Benjamin Van Durme, and Alan Yuille. Localization vs. semantics: Visual representations in unimodal and multimodal models. In *Proceedings of the 18th Conference of the European Chapter of the Association for Computational Linguistics (Volume 1: Long Papers)*, pages 2378–2390, 2024.
- [43] Tristan Thrush, Ryan Jiang, Max Bartolo, Amanpreet Singh, Adina Williams, Douwe Kiela, and Candace Ross. Winoground: Probing vision and language models for visio-linguistic compositionality. In *Proceedings of the IEEE/CVF Conference on Computer Vision and Pattern Recognition*, pages 5238–5248, 2022.
- [44] Matthew Walmer, Saksham Suri, Kamal Gupta, and Abhinav Shrivastava. Teaching matters: Investigating the role of supervision in vision transformers. In *Proceedings of the IEEE/CVF Conference on Computer Vision and Pattern Recognition*, pages 7486–7496, 2023.
- [45] Shilong Liu, Zhaoyang Zeng, Tianhe Ren, Feng Li, Hao Zhang, Jie Yang, Chunyuan Li, Jianwei Yang, Hang Su, Jun Zhu, et al. Grounding dino: Marrying dino with grounded pre-training for open-set object detection. *arXiv preprint arXiv:2303.05499*, 2023.
- [46] Matt Deitke, Dustin Schwenk, Jordi Salvador, Luca Weihs, Oscar Michel, Eli VanderBilt, Ludwig Schmidt, Kiana Ehsani, Aniruddha Kembhavi, and Ali Farhadi. Objaverse: A universe of annotated 3d objects. In *Proceedings of the IEEE/CVF Conference on Computer Vision and Pattern Recognition*, pages 13142–13153, 2023.
- [47] Tsung-Yi Lin, Michael Maire, Serge Belongie, James Hays, Pietro Perona, Deva Ramanan, Piotr Dollár, and C Lawrence Zitnick. Microsoft coco: Common objects in context. In *Computer Vision—ECCV 2014: 13th European Conference, Zurich, Switzerland, September 6–12, 2014, Proceedings, Part V 13*, pages 740–755. Springer, 2014.

- [48] Yining Hong, Haoyu Zhen, Peihao Chen, Shuhong Zheng, Yilun Du, Zhenfang Chen, and Chuang Gan. 3d-llm: Injecting the 3d world into large language models. *Advances in Neural Information Processing Systems*, 36:20482–20494, 2023.
- [49] Kaiming He, Xinlei Chen, Saining Xie, Yanghao Li, Piotr Dollár, and Ross Girshick. Masked autoencoders are scalable vision learners. *arXiv:2111.06377*, 2021.
- [50] René Ranftl, Katrin Lasinger, David Hafner, Konrad Schindler, and Vladlen Koltun. Towards robust monocular depth estimation: Mixing datasets for zero-shot cross-dataset transfer. *IEEE Transactions on Pattern Analysis and Machine Intelligence*, 44(3), 2022.
- [51] Maxime Oquab, Timothée Darcet, Théo Moutakanni, Huy Vo, Marc Szafraniec, Vasil Khalidov, Pierre Fernandez, Daniel Haziza, Francisco Massa, Alaaeldin El-Nouby, et al. Dinov2: Learning robust visual features without supervision. *arXiv preprint arXiv:2304.07193*, 2023.
- [52] Hugo Touvron, Matthieu Cord, and Herve Jegou. Deit iii: Revenge of the vit. *arXiv preprint arXiv:2204.07118*, 2022.

A Details about ImageNet3D Construction

A.1 Dataset Details

Choice of rigid categories. Our goal is to annotate most common rigid categories in natural images. We choose ImageNet21k as the source of our images as it includes a wide range of diverse images with object labels. Given the 21k categories in ImageNet21k, we choose the 200 categories based on the following criteria:

1. **The category must be rigid.** Categories such as animals, clothes, or food are skipped as they are not suitable for category-level pose estimation.
2. **The category must be a general class of objects, rather than a specific and limited subset of objects.** For instance, categories such as Gondola or speed boats are skipped as they are considered as subsets of boats.
3. **The category must have well-defined shapes.** Categories such as chimes vary too much in shapes, making it hard to define common canonical poses for object pose estimation.
4. **Objects from this category must vary in 3D viewpoints.** Images of oscilloscopes are often taken from the same viewpoint (*i.e.*, front), making this category trivial for pose estimation.

Removing ambiguity in 3D viewpoint. Objects from certain categories have ambiguities in terms of 3D viewpoint. For instance, tables when looked from “front” and “back” are visually indistinguishable. Certain datasets resolve this issue by annotating symmetry axes [35]. We follow [13, 24] and resolve the ambiguity by defining a “common” viewpoint. For instance, we assume tables are always looked at from the “front” and bottles always have zero azimuth. Models would learn such biases from the training data and we could adopt the standard pose estimation metrics during evaluation.

For other information, please refer to our [datasheet for dataset](#).

A.2 Annotator Guidelines

To improve the quality of the 3D annotations, we provide detailed guidelines and tutorials to the annotators. These documents provide a detailed introduction to each parameter to be annotated, how to use the web app, and how boundary cases should be handled. We refer the readers to Section D.3 where we provide links to our annotator tutorials and guidelines.

A.3 Caption Generation

In ImageNet3D we provide two types of captions, natural image captions interleaved with 3D information 3.3 and category-level captions that provide detailed descriptions of object shape, part structure, and how humans interact with these objects for all categories in ImageNet3D.

Natural image captions interleaved with 3D information. We follow [6] and adopt a GPT-assisted approach to generate these captions. Specifically, we provide GPT-4v with our 3D annotations as context information and generate natural captions summarizing the objects in the images, as well as the spatial and structural information. To generate captions interleaved with 3D information, we assign names (*e.g.*, CAR1 and BICYCLE1) to each object in the images, which are fed into GPT-4v along with each object’s bounding box. Once we obtain the captions from GPT-4v, we insert 3D annotations after the first mention of the objects names, *i.e.*, from “CAR1” to “CAR1 with <pose6d>”. Please refer to Figure 6 for examples of our system and user prompts.

Category-level captions. We manually annotate category-level captions that describe in details each category’s object shape, part structure, and how humans interact with these objects for all categories in ImageNet3D.

A.4 Ethics and Institutional Review Board (IRB)

We follow the ethics guidelines of NeurIPS and obtained Institutional Review Board (IRB) approvals prior to the start of our work. We described potential risks to the annotators, such as being exposed to inappropriate images from the ImageNet21k dataset [23], and explained the purpose of the study

and how the collected data will be used. All annotators are paid by a fair amount as required at our institution. Link to our IRB approval: drive.google.com.

B Limitations

As our image data are collected from ImageNet21k, most images are object-centric with only one or two instances. Thus our dataset may not be suitable for 3D object detection or tasks that require object co-occurrences. As far as we know, there are no existing 3D object detection datasets with 3D annotations for more than 20 categories. One reason is that annotating 6D poses for multiple categories is very time consuming, and category co-occurrences follow a long-tail distribution. On the other hand, previous studies [32, 33] have found that compositional models trained on object-centric data have the ability to generalize to real images with multiple objects or partial occlusion, which makes our ImageNet3D a competitive option when developing models for general-purpose object-level 3D understanding.

C Implementation Details

C.1 Baseline Models

Classification-based methods. Classification-based methods formulate pose estimation as a classification problem. Three linear classifiers are added on top of feature backbones with respect to the three pose parameters. Continuous values from 0 to 2π are projected into 40 bins, which are then learned with a cross-entropy loss by the classifier heads. All classification-based methods are trained on one A5000 GPUs for less than one day, depending on the backbone size.

3D compositional models. For NOVUM [33], we simply follow the official implementation. For NMM-Sphere, we extend a neural mesh model with a unified sphere mesh shared by all categories. The NMM-Sphere model could be applied for joint classification and pose estimation with a class-contrastive loss, or be used for open-vocabulary pose estimation by learning category-agnostic features. All 3D compositional models are trained on eight A5000 GPUs for about two days.

LLaVA-pose. Similar to [25, 26], we extend the LLaVA [6] model with a <pose> token, which is then decoded with a MLP (*i.e.*, a classifier head) to predict the pose. The LLaVA-pose model is trained on eight A5000 GPUs for one day.

C.2 Training Details

Data augmentations. Our goal is to present baseline performance on ImageNet3D so we avoid complex data augmentations and leave it for future work to explore the benefits of data augmentation. For baseline models on all three tasks, we only adopt random horizontal flip.

Linear probing of object-level 3D awareness. Following [51] we grid search learning rates, pooling strategies, and backbone blocks (where features are taken from) and report the validation accuracy achieved by the best set of parameters.

Open-vocabulary pose estimation. For classification-based methods, models are trained for 120 epochs with a batch size of 64. We adopt the SGD classifier with an initial learning rate of 0.01.

Joint image classification and category-level pose estimation. We adopt the same training strategy as in open-vocabulary pose estimation. Moreover, for weights balancing the classification loss and the pose estimation loss, we simply choose $w_1 = w_2 = 1.0$.

D Data and Code Release

D.1 License

Our ImageNet3D dataset, including 3D and other annotations, are released under the ATTRIBUTION-NONCOMMERCIAL 4.0 INTERNATIONAL license, *i.e.*, [CC BY-NC 4.0](https://creativecommons.org/licenses/by-nc/4.0/). Additionally users should abide to the terms of access and license from the original [ImageNet](https://www.image-net.org/).

D.2 Risks and Concerns

Harmful contents. A very few number of images in ImageNet3D may contain data that, if viewed directly, might be offensive, insulting, threatening, or might otherwise cause anxiety. These images are taken directly from ImageNet21k so please follow the guidelines of [ImageNet21k](#).

Personally identifiable information. Certain images may contain faces to identify individuals. However, these images are taken directly from ImageNet21k so please follow the guidelines of [ImageNet21k](#).

D.3 ImageNet3D Dataset and Code

1. **Datasheet for dataset:** [github.com](#)
2. **Raw data:** [huggingface.co](#)
3. **Croissant metadata:** [huggingface.co](#)
4. **Source code for main experiments:** [github.com](#)
5. **Source code of our web app:** [github.com](#)
6. **Annotator tutorial:** [drive.google.com](#)
7. **Annotator guidelines:** [drive.google.com](#)

E Human Evaluation of Annotation Quality

As there is an overlap of images between ObjectNet3D [24] and ImageNet3D, we analyze the quality of the annotations with human evaluation. Specifically, we present the annotated 6D poses from ObjectNet3D and ImageNet3D side by side to human evaluators. Then the human evaluator must choose which annotation is correct and visually better. The evaluation metrics include both the alignment of 3D viewpoint, as well as the 3D location of the object. We randomly shuffle the order the annotations presented to the annotators.

We collect human evaluation results from 16 categories that are both annotated in ImageNet3D and ObjectNet3D. 50 images are sampled from each category to compare the annotation quality. Results show that for all categories tested, annotations from ImageNet3D are generally favored than the annotations from ObjectNet3D, and on average, for 73.25% of the samples, annotations from ImageNet3D are favored. This demonstrate that 3D annotations from ImageNet3D tend to have a better quality than the annotations in ObjectNet3D. Detailed results are presented in Table 5.

F Additional Experimental Results

F.1 Linear Probing of Object-Level 3D Awareness

We report baseline performance using both $\pi/6$ and $\pi/18$ pose accuracies in Table 6. Moreover, we study the scaling properties of various baseline methods and visualize the results in Figure 7. Results show that DINO v2 and DeiT are not scaling well as model parameters increase, and MAE outperforms DINO v2 in large and huge model sizes.

F.2 Open-Vocabulary Pose Estimation

We report baseline performance using both $\pi/6$ and $\pi/18$ pose accuracies in Table 7.

F.3 Joint Image Classification and Category-Level Pose Estimation

We report baseline performance using $\pi/6$ and $\pi/18$ pose accuracies, as well as the median pose error, in Table 7. Furthermore, we show in Figure 8 the scaling properties of ResNet and Swin Transformer on joint image classification and category-level pose estimation. Results show that Swin Transformer obtains better results when model sizes are comparable to ViT-B but ResNet outperforms Swin Transformer as the model sizes scale up.

Image caption generation with GPT-4v

System:

You are an AI visual assistant that can analyze a single image. You receive an image and a list of main objects, with the object names in the parentheses and object locations in the image given by detailed coordinates. These coordinates are in the form of bounding boxes, represented as (x1, y1, x2, y2) with floating numbers ranging from 0 to 1. These values correspond to the top left x, top left y, bottom right x, and bottom right y.

Using the provided caption and bounding box information, describe the scene in a detailed manner.

When describing the given objects, mention the names of the objects as their reference. Include details like object counts, position of the objects, relative position between the objects.

When using the information from the caption and coordinates, directly explain the scene, and do not mention that the information source is the caption or the bounding box.

User:

Describe the image in details. There are 2 known objects: BICYCLE1 with bounding box [...], and BICYCLE2 with bounding box [...]

Mention the names of the objects as their reference.

GPT-4v:

The image captures a scene of two cyclists participating in a bike race. The cyclist on the right, riding a bicycle BICYCLE1, is at the forefront ... (omitted) The second cyclist, riding a bicycle BICYCLE2, is to the left of the first cyclist and positioned slightly behind ... (omitted) The background shows a dirt pathway with orange mesh barriers on either side and ... (omitted)

Figure 6: **GPT-assisted approach to generate image caption interleaved with 3D information.** Following [6], we provide our 3D annotations and object names as context information to GPT-4v and generate natural image captions interleaved with 3D information. Such captions can be used to integrate general-purpose 3D models with large language models [25, 26].

Category	Ours favored	Category	Ours favored	Category	Ours favored
computer	90%	helmet	56%	coffee maker	66%
mouse	70%	fire extinguisher	66%	backpack	94%
boat	88%	train	64%	piano	76%
bicycle	94%	teapot	56%	suitcase	85%
calculator	74%	flashlight	62%	watch	72%
bucket	60%				

Table 5: **Human evaluation of 3D annotations between ImageNet3D and ObjectNet3D.** For each of the 16 categories, we sample 50 images and present to the annotators to compare the annotation qualities. In this table, we present the percentage of samples where the 3D annotation from ImageNet3D is considered better than the 3D annotation from ObjectNet3D.

Model	Arch.	Supervision	Dataset	Pose Acc@ $\pi/6$							
				Avg.	Elec.	Fur.	Hou.	Mus.	Spo.	Veh.	Work
DeiT III [52]	ViT-B/16	classification	ImageNet21k	36.6	47.9	48.2	36.8	21.5	16.6	35.0	25.3
MAE [49]	ViT-B/16	SSL	ImageNet1k	<u>46.6</u>	<u>57.6</u>	<u>67.8</u>	<u>40.2</u>	<u>29.0</u>	<u>20.2</u>	<u>58.4</u>	25.6
DINO [19]	ViT-B/16	SSL	ImageNet1k	42.0	53.1	57.0	39.8	28.0	19.3	45.3	27.0
DINO v2 [51]	ViT-B/14	SSL	LVD-142M	56.3	64.0	75.3	47.9	32.9	23.5	74.7	38.1
CLIP [20]	ViT-B/16	VLM	<i>private</i>	39.7	50.3	52.8	39.7	23.1	19.3	39.8	26.4
MiDaS [50]	ViT-L/16	depth	MIX-6	40.5	50.9	56.7	<u>40.2</u>	26.7	18.9	39.2	<u>28.1</u>

Model	Arch.	Supervision	Dataset	Pose Acc@ $\pi/18$							
				Avg.	Elec.	Fur.	Hou.	Mus.	Spo.	Veh.	Work
DeiT III [52]	ViT-B/16	classification	ImageNet21k	14.4	19.1	20.4	14.0	7.1	5.9	13.4	11.0
MAE [49]	ViT-B/16	SSL	ImageNet1k	<u>21.7</u>	<u>26.4</u>	<u>35.5</u>	<u>18.1</u>	<u>10.5</u>	7.7	<u>27.1</u>	11.9
DINO [19]	ViT-B/16	SSL	ImageNet1k	18.7	23.2	28.7	16.5	9.3	<u>8.4</u>	20.8	12.3
DINO v2 [51]	ViT-B/14	SSL	LVD-142M	26.1	28.4	40.6	20.6	12.0	9.7	36.3	17.0
CLIP [20]	ViT-B/16	VLM	<i>private</i>	16.8	21.2	25.0	16.0	7.5	6.2	17.2	11.6
MiDaS [50]	ViT-L/16	depth	MIX-6	17.4	22.1	26.7	16.7	8.4	8.1	16.4	<u>12.5</u>

Table 6: **Quantitative results on probing of object-level 3D awareness.** We report the $\pi/6$ pose estimation accuracy for the average performance on all categories, as well as the performance for each meta class (from left to right): *electronics, furniture, household items, music instrument, sports equipment, vehicles & transportation, and work equipment*. Among the tested visual foundation models, DINO v2 demonstrated the best object-level 3D awareness.

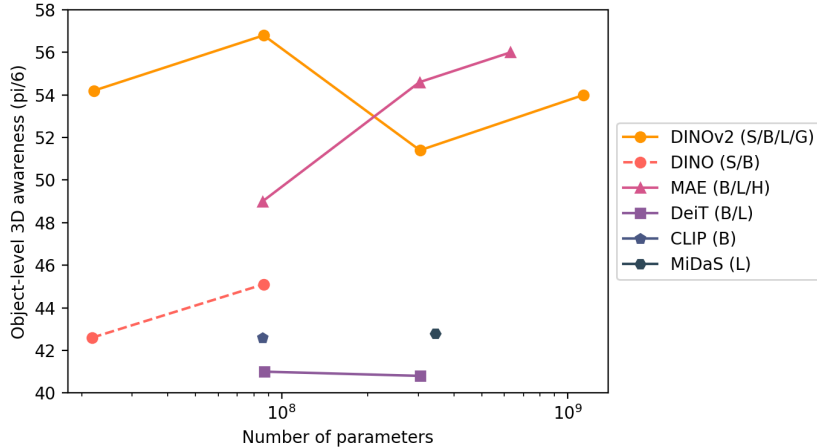


Figure 7: **Scaling properties of various backbones on linear probing of object-level 3D awareness.**

Model	Novel Categories - Pose Acc@ $\pi/6$ \uparrow							
	Avg.	Electronics	Furniture	Household	Music	Sports	Vehicles	Work
ResNet50-General (trained on novel categories)	53.6	49.2	52.4	45.8	26.0	65.2	56.5	58.5
ResNet50-General	37.1	30.1	35.6	28.1	11.8	51.7	36.7	40.9
SwinTrans-T-General	<u>35.8</u>	<u>30.9</u>	<u>34.3</u>	<u>26.1</u>	<u>12.2</u>	<u>46.2</u>	<u>34.4</u>	<u>39.2</u>
NMM-Sphere	29.5	31.7	25.4	21.7	25.6	19.8	33.4	19.3

Model	Novel Categories - Pose Acc@ $\pi/18$ \uparrow							
	Avg.	Electronics	Furniture	Household	Music	Sports	Vehicles	Work
ResNet50-General (trained on novel categories)	25.5	25.9	23.3	19.2	11.8	31.0	27.4	28.2
ResNet50-General	13.5	13.2	<u>12.4</u>	9.0	<u>2.1</u>	21.8	13.1	15.0
SwinTrans-T-General	<u>13.1</u>	13.2	12.7	<u>8.1</u>	1.7	<u>18.0</u>	<u>11.9</u>	<u>13.6</u>
NMM-Sphere	6.0	6.6	4.4	3.5	3.1	4.7	6.2	2.8

Table 7: **Quantitative results on open-vocabulary pose estimation.** We report the *pose estimation accuracy* with threshold $\pi/6$ on testing data from novel categories unseen during training. We report the average performance on all novel categories, as well as performance for novel categories in each meta class. Results show that models with category-agnostic features can generalize to novel categories, but by a limited amount.

Model	3D-Aware Acc@ $\pi/6$ \uparrow							
	Avg.	Electronics	Furniture	Household	Music	Sports	Vehicles	Work
ResNet50-General	50.9	60.0	<u>67.2</u>	43.0	43.8	27.7	64.1	33.8
SwinTrans-T-General	53.2	63.1	71.6	44.8	<u>45.3</u>	30.4	66.2	35.0
LLaVA-pose	49.1	58.0	65.6	41.6	41.0	26.1	61.8	32.1
NOVUM [33]	<u>56.2</u>	59.6	65.6	52.5	41.9	<u>30.6</u>	69.6	<u>39.3</u>
NMM-Sphere	57.4	<u>61.3</u>	65.9	<u>52.4</u>	51.7	40.5	<u>67.9</u>	43.4

Model	3D-Aware Acc@ $\pi/18$ \uparrow							
	Avg.	Electronics	Furniture	Household	Music	Sports	Vehicles	Work
ResNet50-General	<u>25.3</u>	<u>28.6</u>	<u>35.5</u>	19.0	<u>16.3</u>	<u>13.2</u>	<u>36.1</u>	<u>16.2</u>
SwinTrans-T-General	27.4	31.2	40.1	<u>19.9</u>	19.3	15.4	39.2	16.9
LLaVA-pose	15.2	16.2	20.5	11.7	10.8	9.0	23.0	9.2
NOVUM [33]	21.7	22.5	26.2	18.4	10.5	6.6	33.8	9.5
NMM-Sphere	22.8	23.2	31.4	20.1	14.5	10.7	32.7	9.2

Model	Median Pose Error \downarrow							
	Avg.	Electronics	Furniture	Household	Music	Sports	Vehicles	Work
ResNet50-General	28.6	<u>19.6</u>	<u>14.5</u>	46.9	38.0	88.5	16.3	67.5
SwinTrans-T-General	25.6	17.1	12.4	40.8	<u>35.4</u>	68.0	14.7	64.5
LLaVA-pose	31.2	22.5	17.3	49.5	40.7	90.3	19.1	70.1
NOVUM [33]	<u>24.4</u>	22.1	18.6	27.6	35.7	<u>58.1</u>	<u>16.0</u>	<u>41.6</u>
NMM-Sphere	23.7	21.4	17.4	27.6	28.7	43.4	17.0	36.2

Table 8: **Quantitative results on joint image classification and category-level pose estimation.** We report the *3D-aware classification accuracy* with threshold $\pi/6$ for the average performance, as well as performance for each meta class. Results show that with ImageNet3D, we can develop unified 3D models capable of inferring 3D information for a wide range of rigid categories. However, we also identify limitations of current 3D models when scaling up to a lot more object categories.

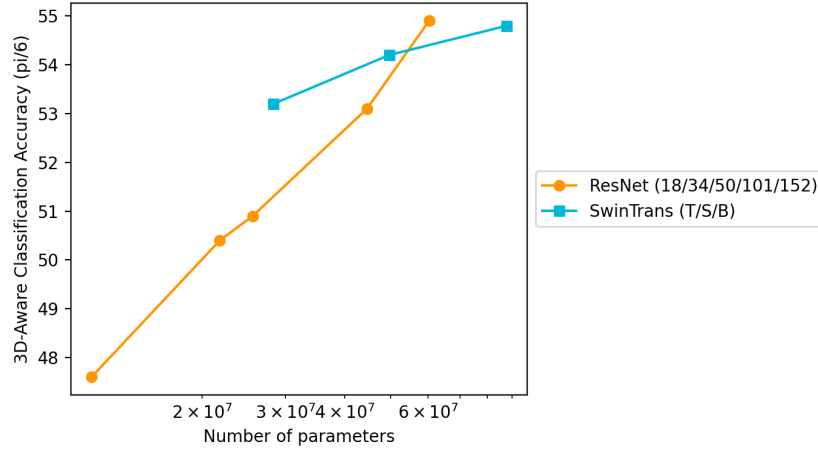


Figure 8: **Scaling properties of ResNet-50 and Swin Transformer on joint image classification and category-level pose estimation.**